MHD modeling of the Effect on n=2 RMP on Peeling-Ballooning mode in KSTAR

S.K. Kim[1], S. Pamela[2], O. Kwon[3], M. Becoulet[4], G. Huijsmans[4], M. Hoelzl[5], Y. In[6], J.H. Lee[7], M. Kim[7], J.K. Park[8], N. Logan[8], S.M. Yang[8], JOREK team and Yong-Su Na[1]

[1] *Department of Energy System Engineering, Seoul National University, Korea*
[2] *Culham Centre for Fusion Energy, CCFE, UK*
[3] *Department of Physics, and Department of Materials-Energy Science and Engineering, Daegu University, Korea*
[4] *Department of plasma physics, CEA, France*
[5] *Max Plank Institute for Plasma Physics, Garching, Germany*
[6] *Department of Physics, UNIST, Korea*
[7] *National Fusion Research Institute, Korea*
[8] *Princeton Plasma Physics Laboratory, USA*

Plasma Laboratory for Advanced REsearch

SEOUL NATIONAL UNIVERSITY

E-mail: ksk911211@snu.ac.kr

2020.03.02

National Fusion Research Institute

Outline

- **Introduction**
- **Simulation setup**
  - Numerical tools & Reference
- **RMP driven Plasma response**
  - Kink-tearing response
  - Increased pedestal transport
- **RMP driven ELM crash suppression**
  - Natural & RMP PBM simulation
  - Coupled RMP & PBM
  - PBM locking
- **Conclusion**

RMP simulation with equilibrium — - Equilibrium response

↓

Natural PBM (w/o RMP) simulation
RMP simulation with PBM — - PBM response

RMP driven ELM suppression

- **RMP driven ELM crash suppression**
  - ✓ **Peeling-ballooning mode (PBM) [1,2] is the main instability resulting in large ELMs.**
  - ✓ **Resonant MP (RMP) can suppress the ELM crash [3-5].**
  - ✓ **Suppression has a very narrow operation window [6].**
    - ➢ **Mechanism is important for reliable ELM control**

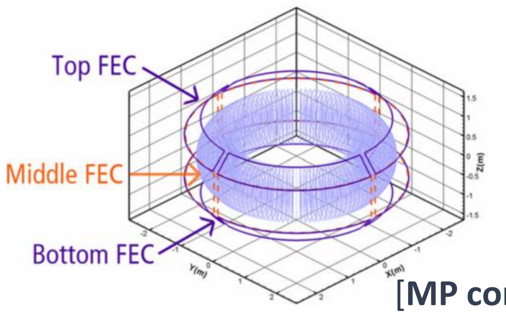

[**MP configuration (KSTAR)**, D. Kim (PPCF 2010)]

- **Increased pedestal transport by RMP application**
  - ✓ **RMP can increase the radial transport of the pedestal.**
  - ✓ **It can degrade the pedestal gradient by forming the stochastic layer [7-9].**

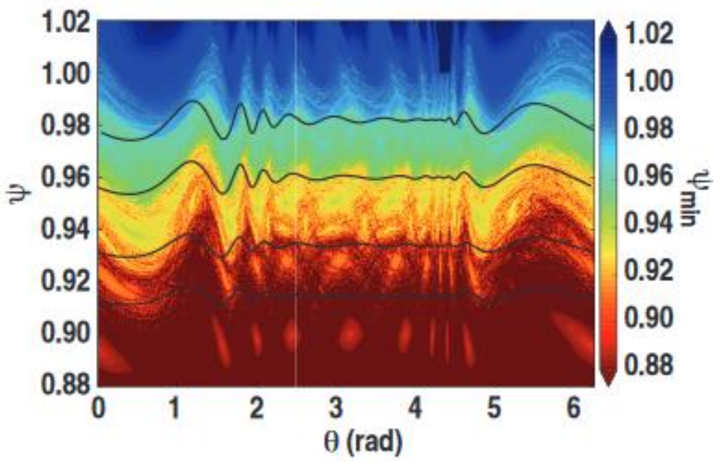

[**RMP driven stochastic layer**, A. Wingen (PPCF 2015)]

[1] J. W. Connor, PPCF 40 (1998), 191
[2] P. B. Snyder et al., NF 44(2004), 320
[3] T. E. Evans et al., PRL 92(2004), 0235003
[4] W. Suttrop et al., PRL 106 (2011), 225004
[5] Y. M. Jeon et al., PRL 109 (2012), 035004
[6] J. K. Park et al., Nature Physics 14 (2018), 1223
[7] R. Fitzpatrick et al., POP 5 (1998), 3325
[8] M. Heyn et al., NF 54 (2014), 064005
[9] N.M. Ferraro et al., POP 19 (2012), 056105

RMP driven ELM suppression

- "Initial" understanding of RMP driven ELM suppression

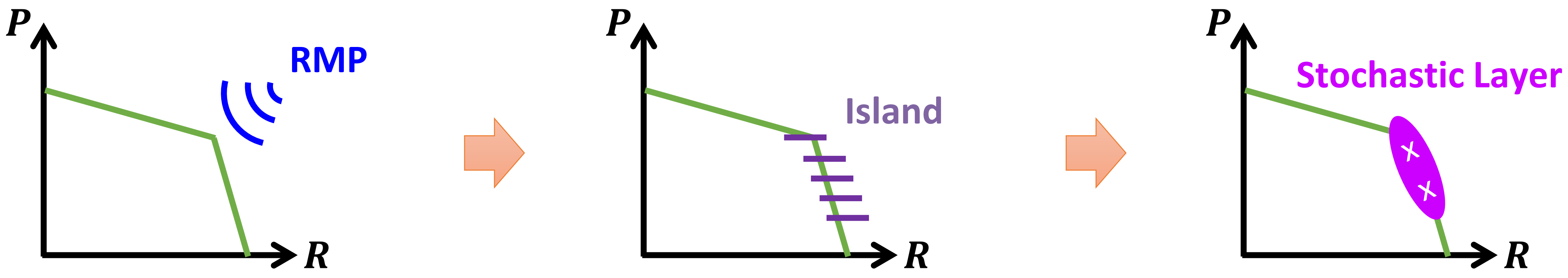

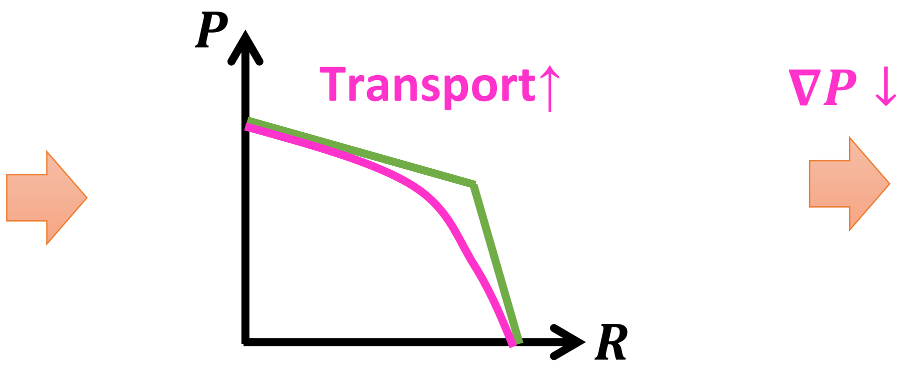

Linearly Stable to PBM

→ No ELM ☺

Possible limits of ‘initial’ explanation

- **Interesting features in RMP driven ELM crash suppression**
  - ✓ **PBM-like filaments remain during the suppression phase [1,2].**
  - ✓ **Mode structure is locked when suppression is achieved.**
  - ✓ **Experimental observation found the importance of $\omega_{\perp,\mathbf{E}\times\mathbf{B}} \approx 0$ [3].**

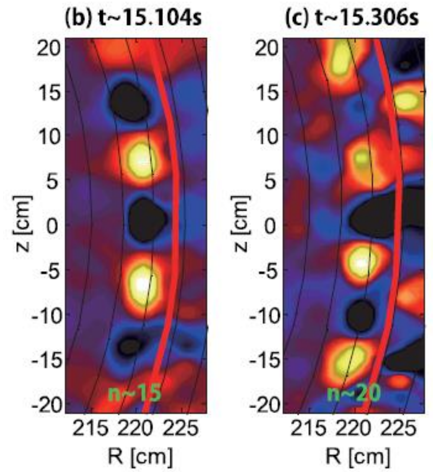

[**2D-ECEI,** J.Lee (PRL 2016)]

Missing keys ?
- **Role of micro-instabilities**
- **Role of MHD characteristics**

→ This study is focused on MHD behavior

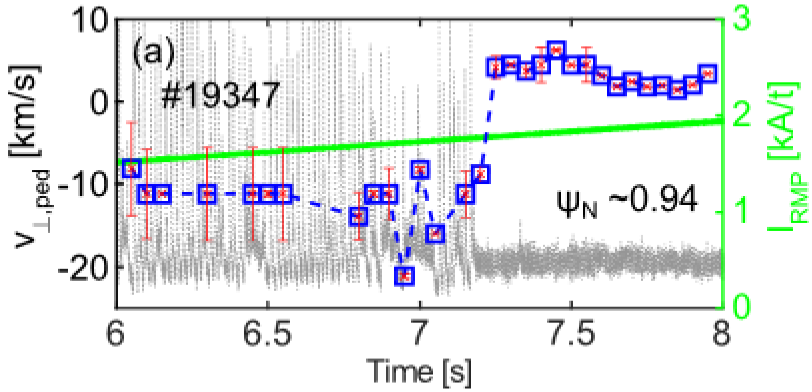

[**Mode rot. bifurcation in suppression,** J.Lee (NF 2019)]

➢ **NL simulation including both RMP and PBM is conducted.**

[1] J. Lee et al., PRL 117 (2016), 075001
[2] J. Lee et al., NF 59 (2019), 066033
[3] C. Paz-Soldan et al., NF 59 (2019), 056012

Outline

- Introduction
- Simulation setup
  - Numerical tools & Reference
- RMP driven Plasma response
  - Kink-tearing response
  - Increased pedestal transport
- RMP driven ELM crash suppression
  - Natural & RMP PBM simulation
  - Coupled RMP & PBM
  - PBM locking
- Conclusion

RMP simulation with equilibrium — - Equilibrium response

⬇

Natural PBM (w/o RMP) simulation
RMP simulation with PBM — - PBM response

Numerical tools

- **JOREK (3D Nonlinear MHD simulation code) [1]**
  - ✓ **Toroidal X-point geometries with scrape-off layer is included.**
  - ✓ **4-fields Reduced MHD equation [2] is used.**

$$\boxed{\frac{1}{R^2}\frac{\partial \psi}{\partial t} = \eta(T)\nabla\cdot\left(\frac{1}{R^2}\nabla_\perp\psi\right) - \vec{B}\cdot\left(\nabla u - \tau_{\mathrm{IC}}\frac{\nabla p_{\mathrm{e}}}{\rho}\right)}$$

Ohm's law

$$\boxed{\frac{\partial \rho}{\partial t} = -\nabla\cdot(\rho\vec{v}) + \nabla\cdot(D\nabla\rho) + S_{\rho}}$$

Continuity eqn.

$$\boxed{\rho\left(\frac{\partial}{\partial t} + \vec{v}\cdot\nabla\right)(\vec{v}_{\mathrm{E}} + \vec{v}_{||}) = -\nabla(\rho T) + \vec{J}\times\vec{B} + S_{\mathrm{v}} - \vec{v}S_{\rho} + \mu\Delta\vec{v} - \nabla\cdot\overleftrightarrow{\Pi}_{\mathrm{neo}}}$$

Ion Momentum eqn.

$$\boxed{\frac{\partial(\rho T)}{\partial t} = -(\vec{v}_{\mathrm{E}} + \vec{v}_{||})\cdot\nabla\rho T - \gamma\rho T\,\nabla\cdot(\vec{v}_{\mathrm{E}} + \vec{v}_{||}) + \nabla\cdot(\kappa\nabla T) + (1-\gamma)S_{\mathrm{T}}}$$

Energy eqn.

$$\boxed{\vec{v} = \vec{v}_{\mathrm{E}} + \vec{v}_{\mathrm{i*}} + \vec{v}_{||}}$$

Fluid model is included

w/ toroidal rotation
w/ diamagnetic effect
w/ neoclassical viscosity

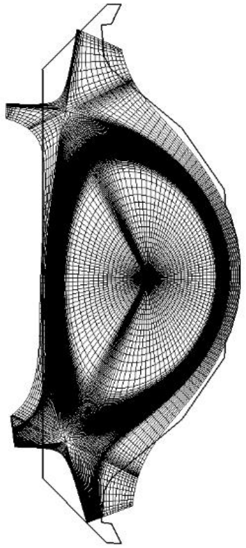

[**JOREK grid for KSTAR**]

- **ERGOS (Vacuum RMP field code) [3]**
  - ✓ **Vacuum MP is calculated.**

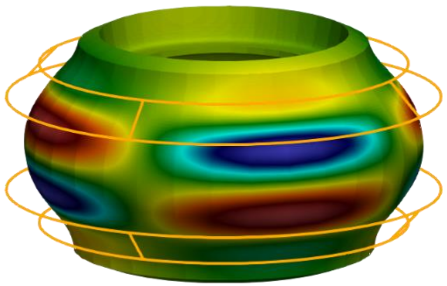

[**RMP on JOREK boundary for KSTAR,** ERGOS]

[1] G. T. A Huysmans et al, PPCF 51 (2009), 124012
[2] F. Orain et al., POP 20 (2013), 102510
[3] M. Becoulet et al., Nucl. Fusion 48 (2008), 024003

Reference plasma

- **Target discharge and equilibrium**
  - ✓ **ELM suppression discharge (#18594) [1] of KSTAR is selected**
  - ✓ $B_T = 1.8$ T, $I_p = 660$ kA, $q_0 \sim 1$, $q_{95} \sim 4$, $\beta_p = 1.0$, $\bar{n}_e = 3.3 \times 10^{19}$ m^{-3}
  - ✓ **ELM suppression is achieved with n=2 ($\phi = 90°$), $I_{RMP} \sim 3.7$kA RMP configuration [2].**

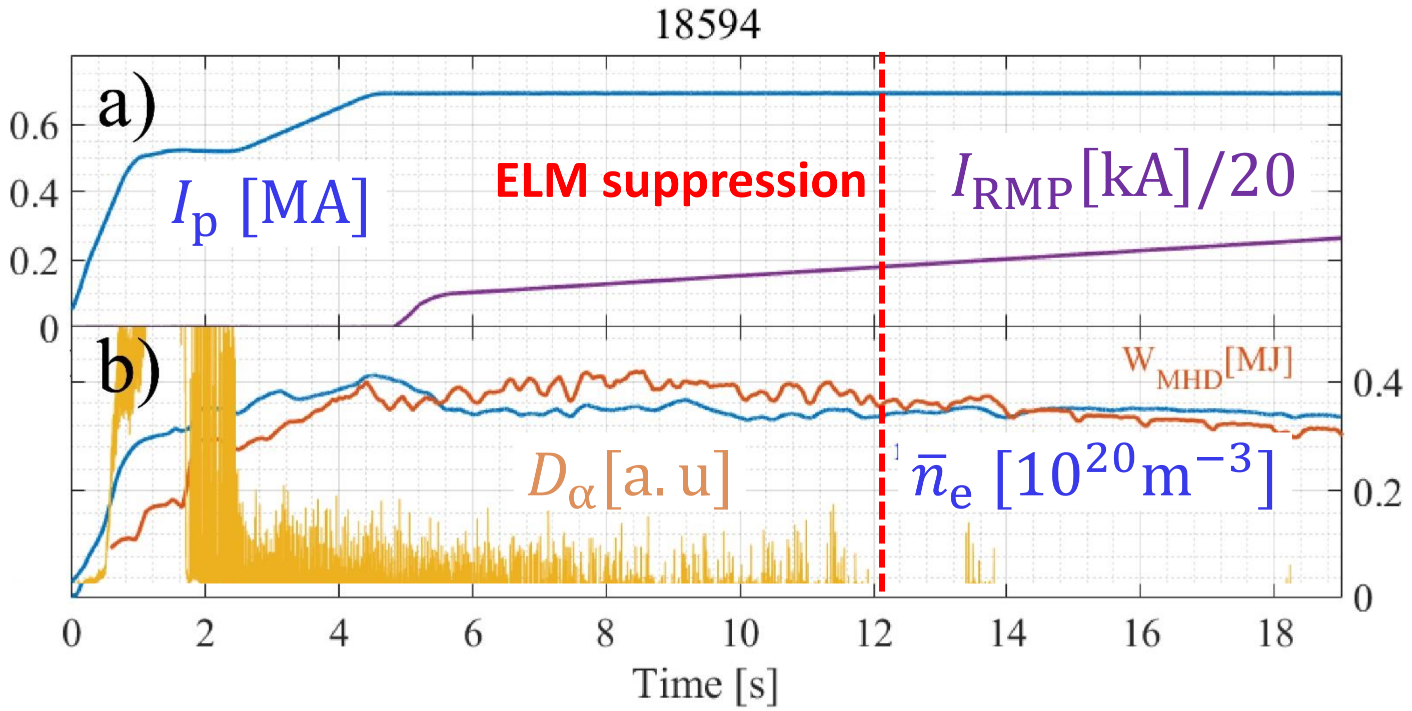

[#18594 overview]

[1] J. Lee et al., Nucl. Fusion (2019), 066033
[2] Y. M. Jeon et al., PRL 109 (2012), 035004

Reference plasma - Profile & EFIT

- **Kinetic profile and EFIT construction**
  - ✓ We developed GFIT & GEFIT package to construct a kinetic profile and EFIT in KSTAR.
  - ✓ Numerical/Theoretical corrections are applied to solve obstacles in theses constructions.
  - ✓ They are in full operation at the KSTAR computing server (one of the standard tool).

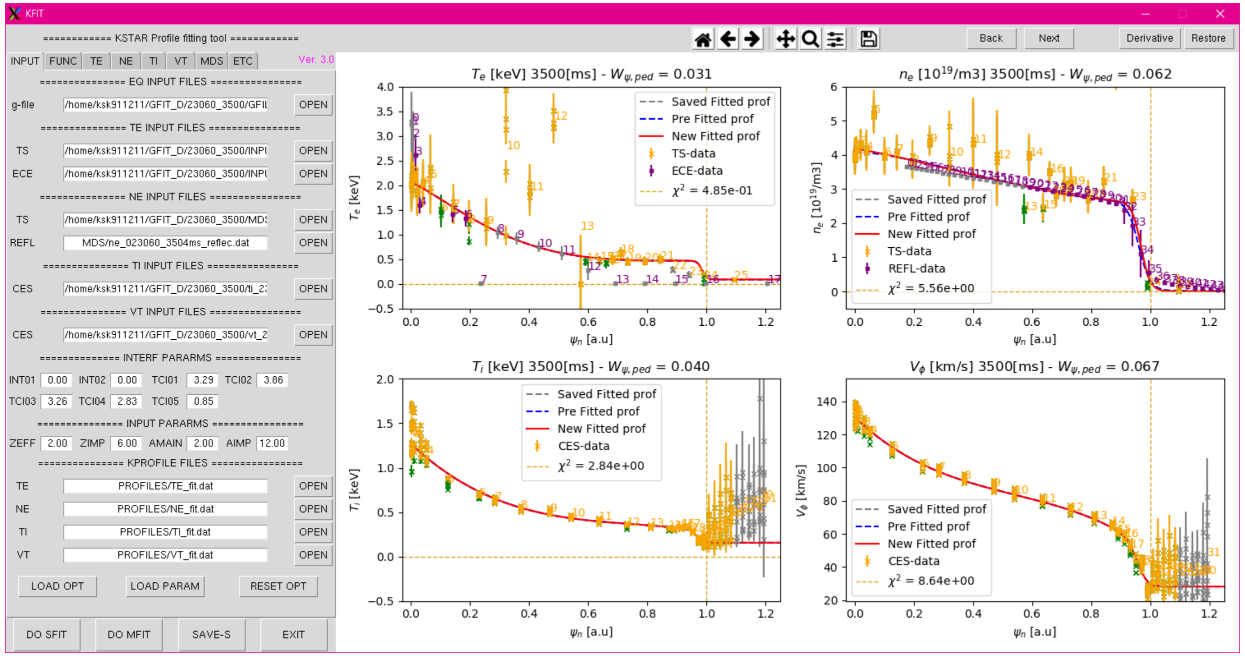

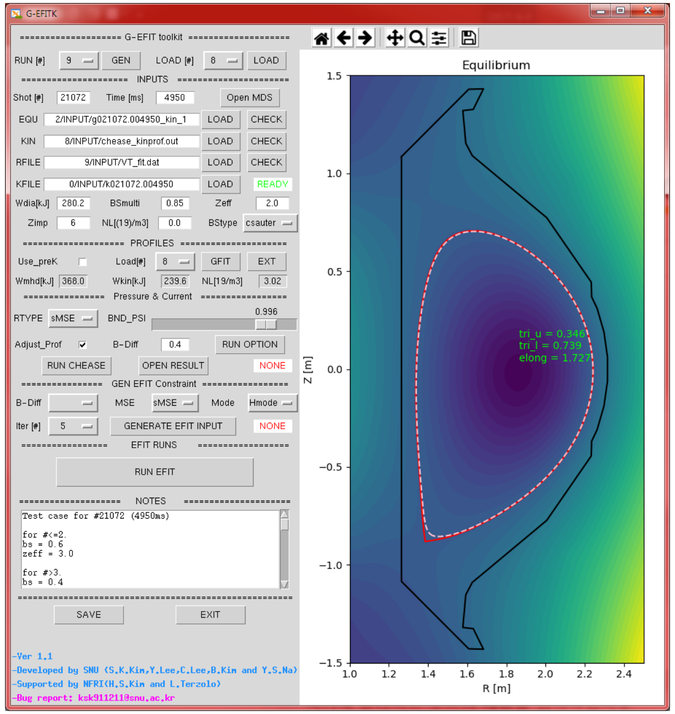

[GFIT & GEFIT package, KSTAR]

Outline

- Introduction
- Simulation setup
  - Numerical tools & Reference
- RMP driven Plasma response
  - Kink-tearing response
  - Increased pedestal transport
- RMP driven ELM crash suppression
  - Natural & RMP PBM simulation
  - Coupled RMP & PBM
  - PBM locking
- Conclusion

RMP simulation with equilibrium — - Equilibrium response

⬇

Natural PBM (w/o RMP) simulation
RMP simulation with PBM — - PBM response

RMP driven Plasma response - Approach

- **Numerical modeling of MP application**
  - ✓ **Boundary condition is modified with vacuum RMP field ($\delta\psi_{\mathrm{pol,RMP}}$).**

$$\psi_{\mathrm{bdy}} = \psi_{\mathrm{bdy,0}} + \delta\psi_{\mathrm{bdy,RMP}}$$

  - ✓ **Vacuum field approximation is used on the boundary.**
  - ✓ **Field penetration and the response (only n=0 & 2) are self-consistently calculated.**

  ➢ **Kink-tearing response is reproduced.**

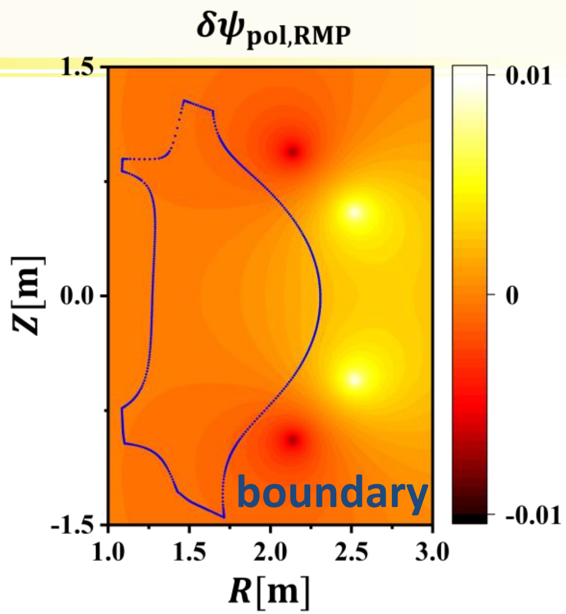

[$\delta\psi_{\mathrm{pol,RMP}}$ in the simulation]

Kink-tearing response - Kink

- **Kink response**

Kink
- ✓ It has an edge localized structure.
- ✓ It has large deformation at X-point.

- ✓ It results in a $v_{E\times B}$ convection layer on the pedestal.

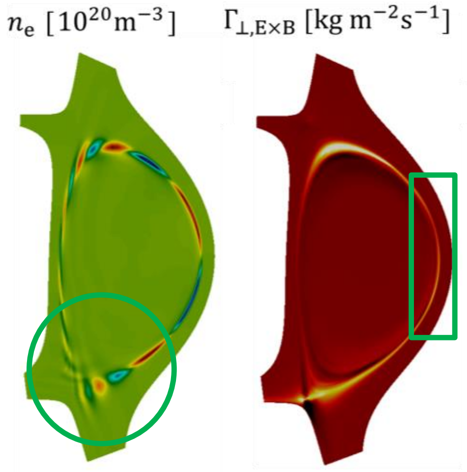

[Kink-peeling response]

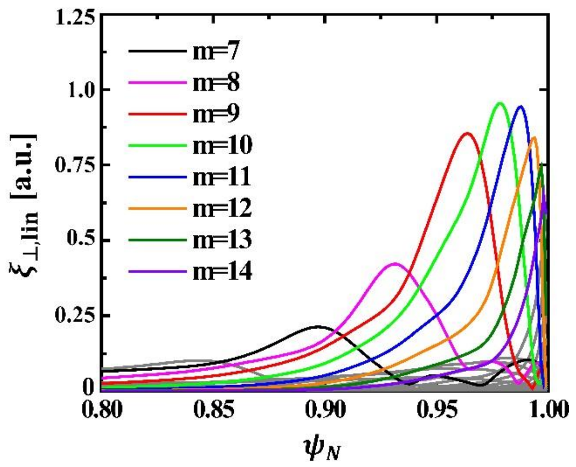

[Kink-peeling structure]

Plasma response - Tearing

- **Tearing response**

Tearing
- ✓ Perturbed current shields the external field.
- ✓ $v_{\perp e} \approx 0$ layer and finite resistivity in the edge weaken the field shielding.
- ✓ Field penetration occurs in the pedestal region.
- ✓ As a result, stochastic layer is formed.

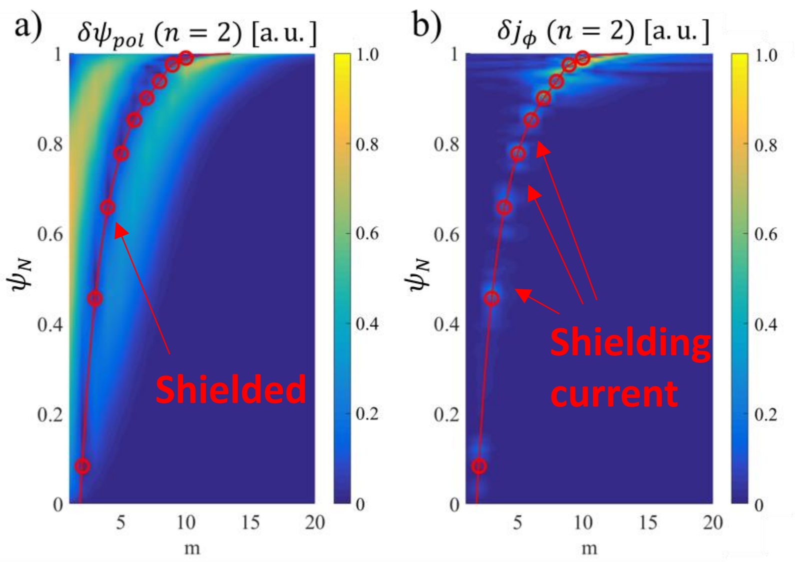

[Fourier plot for $\delta\psi_{\mathrm{pol}}$ and δj_ϕ for n=2]

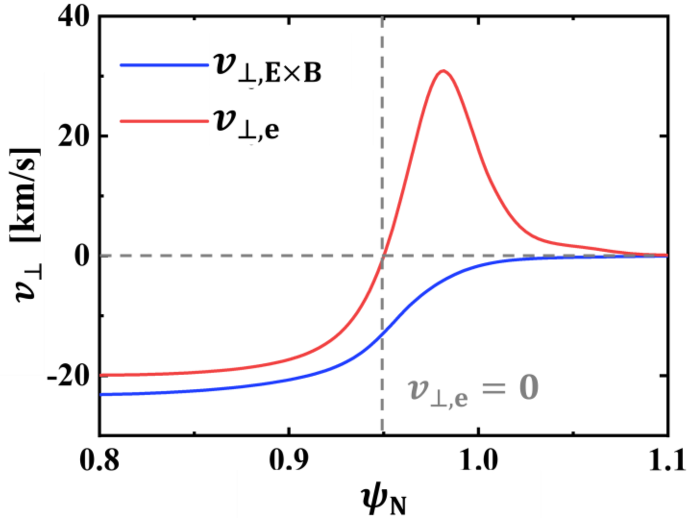

[Perpendicular flow profile]

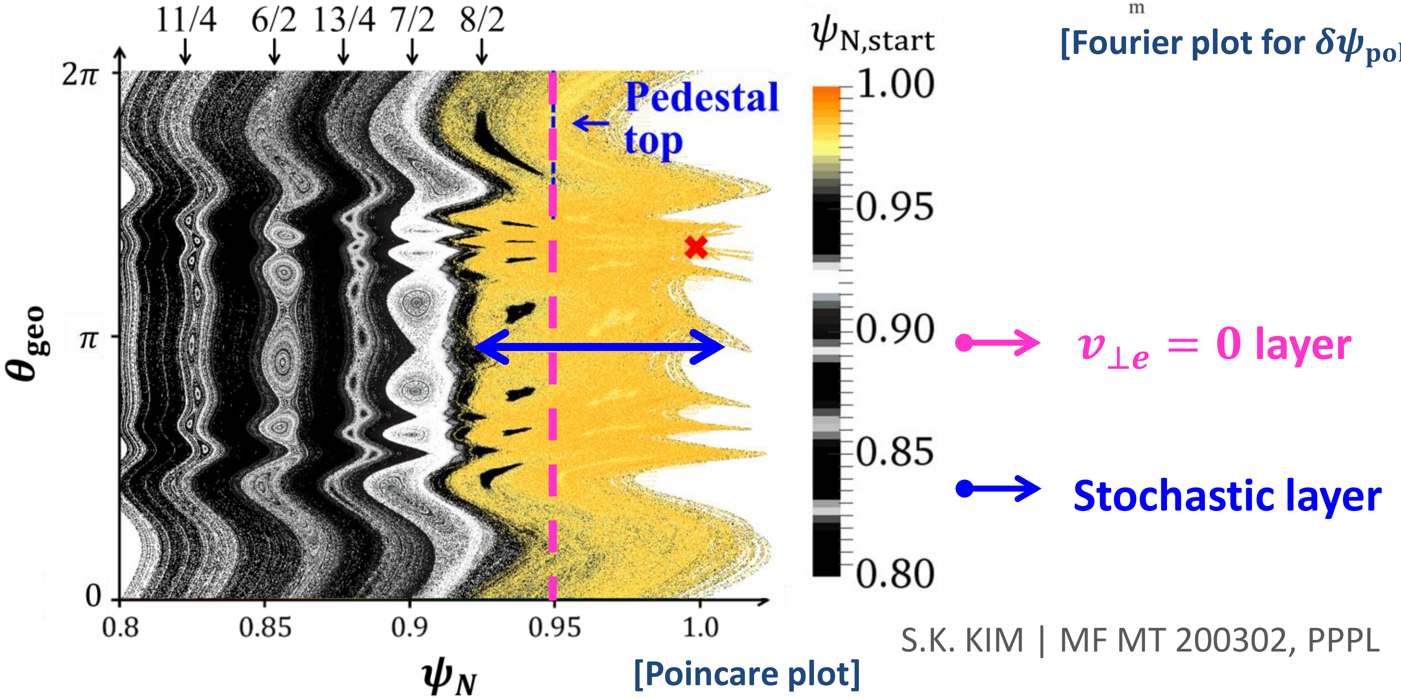

[Poincare plot]

Increased pedestal transport - Agreement

- **Pedestal profile degradation**
  - ✓ Radial transport increases due to
    - $v_{\mathbf{E}\times\mathbf{B}\perp}$ convection (Kink).
    - Stochastic layer (Tearing).
  - ✓ Pedestal profile (n=0) is degraded.
  - ✓ Density pedestal is governed by $v_{\mathbf{E}\times\mathbf{B},\perp}$.
  - ✓ It is consistent with the trend that density pump-out increases with kink response [1,2].
  - ✓ T pedestal shows a similar tendency in the experiment and simulation.
  - ✓ However, the decrease in $\bar{n}_e$ from the experiment is three times larger than the simulation.

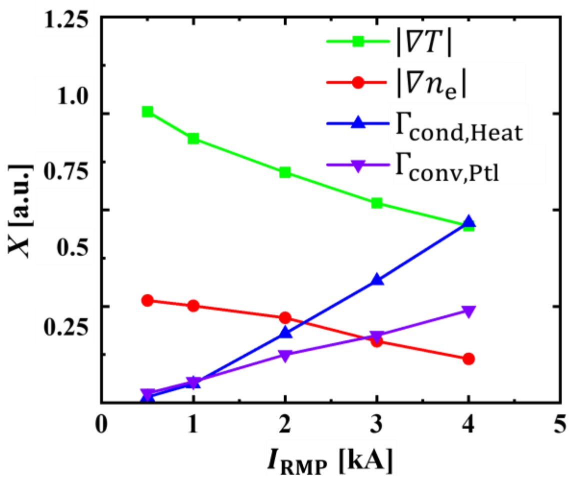

[Radial fluxes vs $I_{\rm RMP}$]

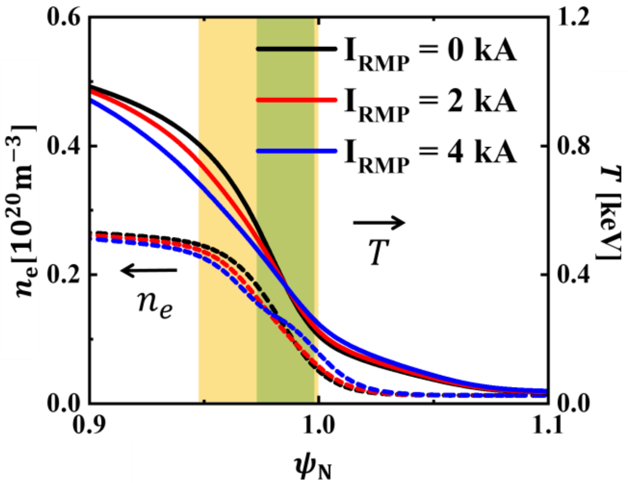

[Pedestal degradation vs $I_{\rm RMP}$]

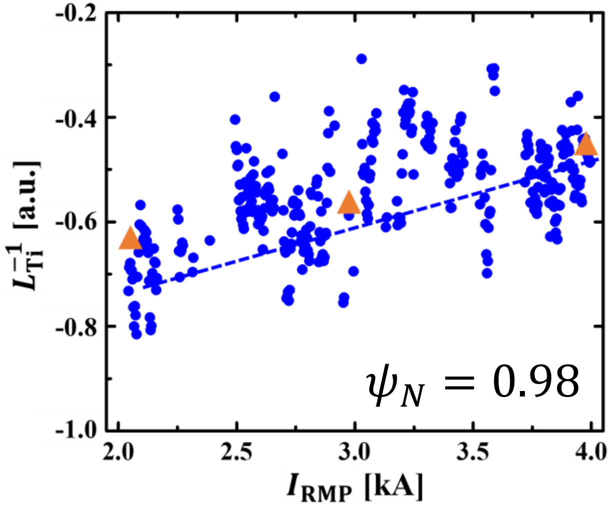

[$L_{\rm Ti}^{-1}$ vs $I_{\rm RMP}$]

[1] Y. Liu et al., PPCF 58 (2016), 114005
[2] C. Paz-Soldan et al., Nucl. Fusion (2016), 056001

Increased pedestal transport - Disagreement

- **Pedestal profile degradation**
  - ✓ Change in V_ϕ pedestal is also not consistent.
  - ✓ This study does not include
    - Effect of micro-instability [1-4]
    - Magnetic flutter [5] and proper transport model [6]
    - Neoclassical Toroidal Viscosity (NTV) [7,8]
  - ✓ $\Gamma_{\mathrm{E\times B,MHD}}$ can not solely explain the pump-out.
    → Role of NTV and micro instability is also important.
    - ➢ These transport mechanisms will be needed to fully explain the RMP driven profile degradation.
  - ✓ The linear growth rate of PBM decreases with pedestal gradient.

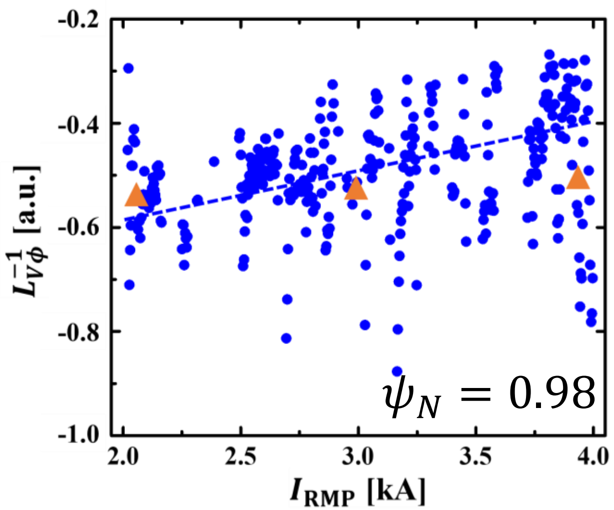

[$L_{\mathrm{V}\phi}^{-1}$ vs I_{RMP}]

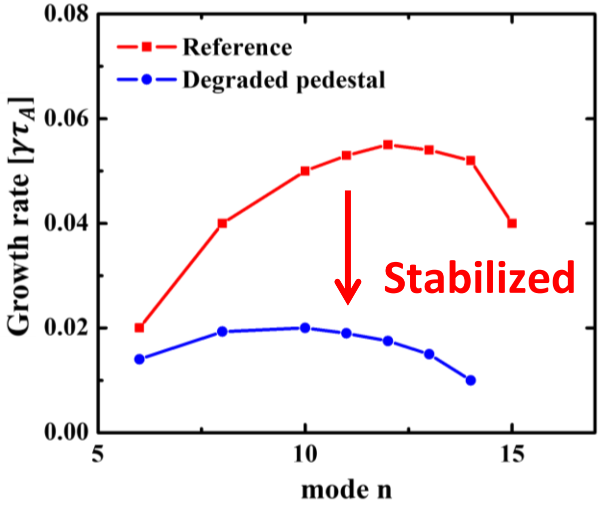

[Growth rate spectrum]

[1] T.M. Bird et al., NF 53 (2013), 013004
[2] I. Holod et al., NF 57 (2017), 016005
[3] G.J. Choi and T.S. Hahm NF 58 (2018), 026001
[4] R. Hager et al., APS-DPP (2019), Florida, USA
[5]F.L. Waelbroeck et al., NF 52 (2012), 074004
[6] T. Rhee et al., NF 55 (2015), 032004
[7] W. Zhu et al., PRL 96 (2006), 225002
[8] J.-K. Park et al., POP 16 (2009), 056115

Outline

- Introduction
- Simulation setup
  - Numerical tools & Reference
- RMP driven Plasma response
  - Kink-tearing response
  - Increased pedestal transport
- RMP driven ELM crash suppression
  - Natural & RMP PBM simulation
  - Coupled RMP & PBM
  - PBM locking
- Conclusion

RMP simulation with equilibrium - Equilibrium response

⬇

Natural PBM (w/o RMP) simulation

RMP simulation with PBM - PBM response

Natural PBM simulation (without RMP)

- **Linear PBM simulation**
  - ✓ Linearly dominant n is $n_{\mathrm{ECEI}} = 11 \pm 1, n_{\mathrm{sim}} = 12$.
  - ✓ Poloidal velocity of mode is $v_{\theta,\mathrm{mode}} \sim 3\ \mathrm{km/s}$ in both cases (ECEI & simulation).
  - ✓ $v_{\theta,\mathrm{mode}} \approx v_{\theta,E\times B}$ (LAB, ion - diamagnetic direction) [1,2].

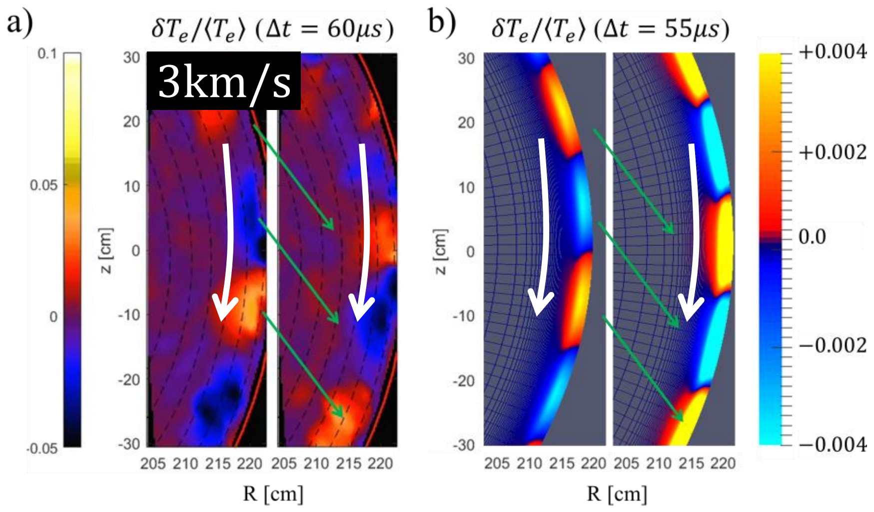

[ECEI and JOREK n=12 results]

- **Nonlinear PBM calculation**
  - ✓ Mode crash is reproduced during nonlinear phase.
  - ✓ Large heat flux occurs with pedestal collapse.
  - ✓ $\Delta W_{\mathrm{ELM,sim}} \approx 8\mathrm{kJ}$ ($\Delta W_{\mathrm{ELM,exp}} \approx 7 \pm 4\mathrm{kJ}$).

➢ Experimentally relevant ELM with $v_{\theta,\mathrm{mode}} \approx v_{\theta,E\times B}$ is obtained.

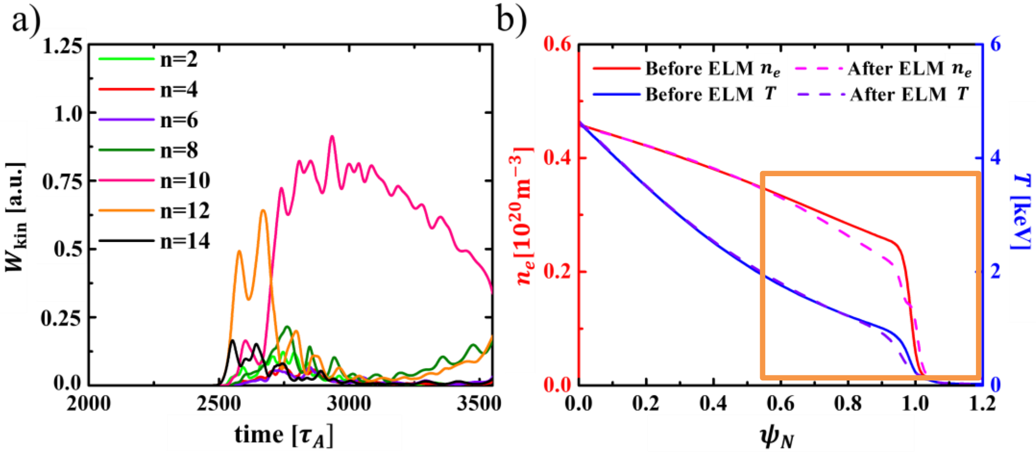

[Mode amplitude in NL phase] [Pedestal degradation after ELM]

[1] Morales J. 2016 Phys. Plasmas 23 042513
[2] Becoulet M. et al 2017 Nucl. Fusion 57 116059

RMP-PBM simulation

- **Effect of RMP on PBM**
  - ✓ **PBMs are affected by RMP driven plasma response via mode coupling.**
  - ✓ **Mode mitigation occurs with small I_{RMP} ($\lesssim$ 2kA).**
  - ✓ **Mode crash suppression is achieved with $I_{\mathrm{RMP}} \sim$ 4 kA (~3.7 kA in exp.).**
  - ✓ **PBM suppression is reproduced with experimentally relevant RMP.**
    - ➢ **Mode suppression can be related to the reduced pedestal gradient.**

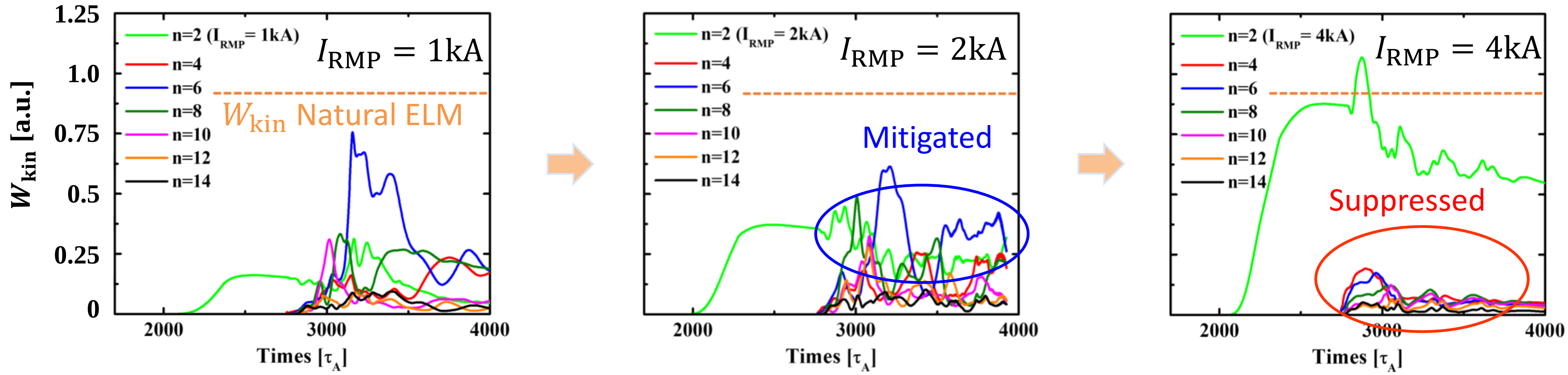

[Nonlinear evolution of MHD modes with RMPs]

Coupled RMP & PBM

- **Comparison between w/ and w/o mode coupling case**

  ✓ **Degraded pedestal due to RMP ($I_{\mathrm{RMP}} = 4\mathrm{kA}$) is included in both cases.**

  ✓ **Nonlinear PBM simulation w/o mode couplings shows**

  - A bursty behavior in its nonlinear phase

  ✓ **Nonlinear PBM simulation w/ mode couplings shows**

  - Mode suppression without bursty behavior

  ✓ **Therefore, suppression of PBM with RMP is related to both**

  - Reduced pressure gradient

  - Coupling of PBMs and RMP driven plasma response

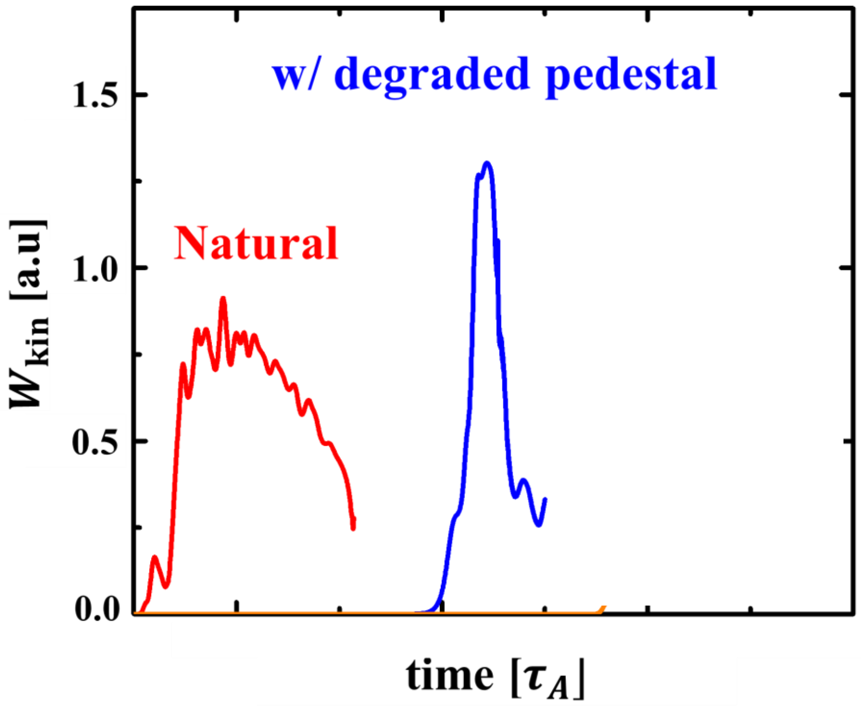

[Mode amplitude of PBM with n=10]

Coupled RMP & PBM

- **Increased transport with coupled RMP-PBM**

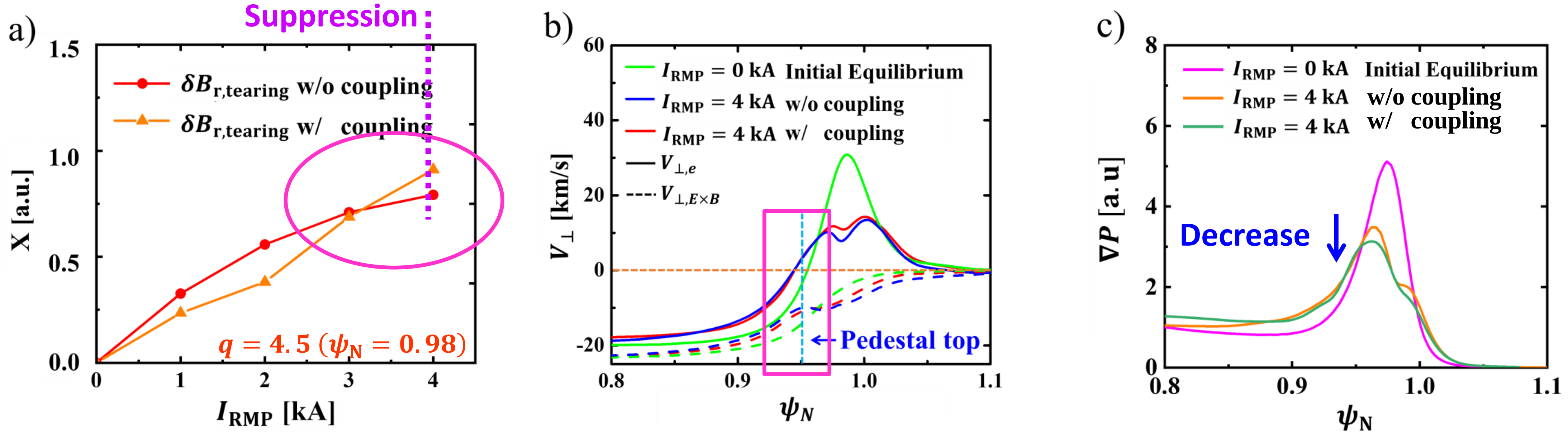

✓ **Tearing component decrease with the mode coupling effect for $I_{RMP} \leq 2$ kA.**

✓ **Magnetic island is amplified under the coupling effect when suppression is achieved.**

✓ **Effect of mode coupling on the perpendicular flow is small.**

✓ **Pedestal transport is increased by the coupling effect.**

- **Larger stochastic layer and pedestal transport**
- **Smaller pedestal gradient (Reduced instability source)**

Coupled RMP & PBM

- **Increased energy transfer with coupled RMP-PBM**

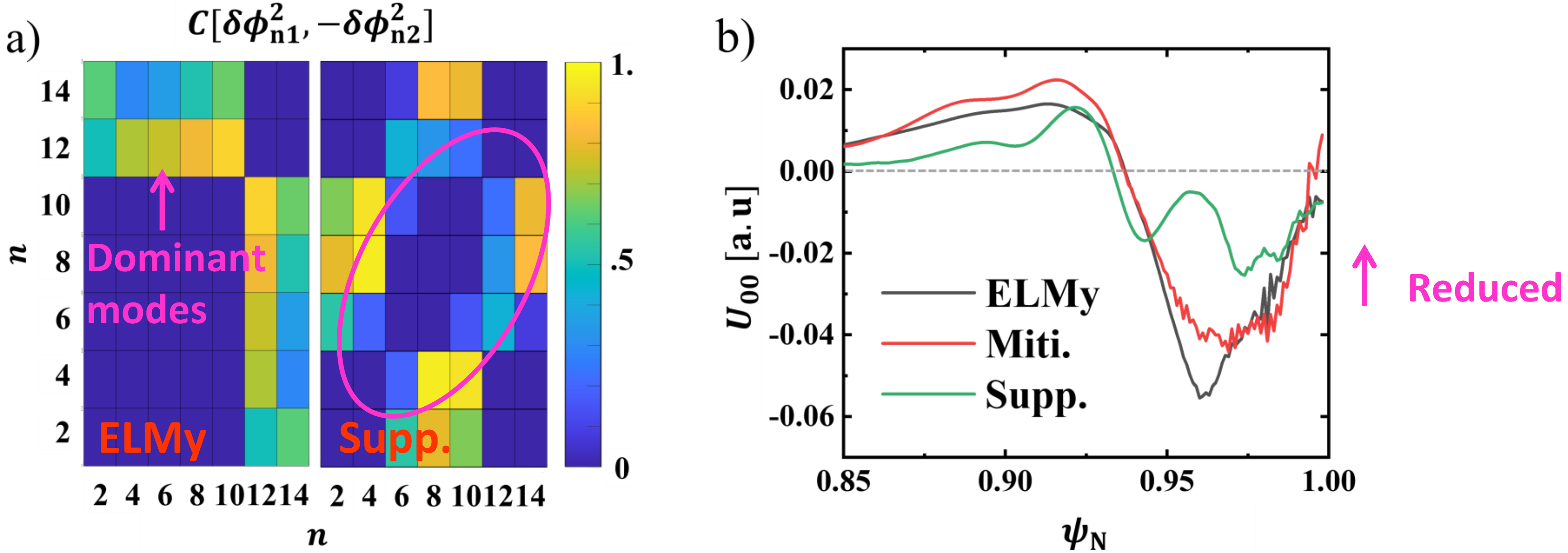

✓ **Interaction between harmonics increases [1] with RMP.**

- **Amplified energy transfer between harmonics**

✓ **Vorticity U_{00} in the pedestal is reduced.**

- **More evenly distributed perturbed energy among harmonics [2]**

✓ **Catastrophic growth of unstable mode can be prevented [3].**

[1] M. Becoulet et al., PRL 113 (2014), 115001
[2] H. Jhang et al., NF 57 (2017), 022006
[3] P.W. Xi et al., PRL 112 (2014), 085001

Coupled RMP & PBM - Suggestion

- **Effect of coupled RMP-PBM**

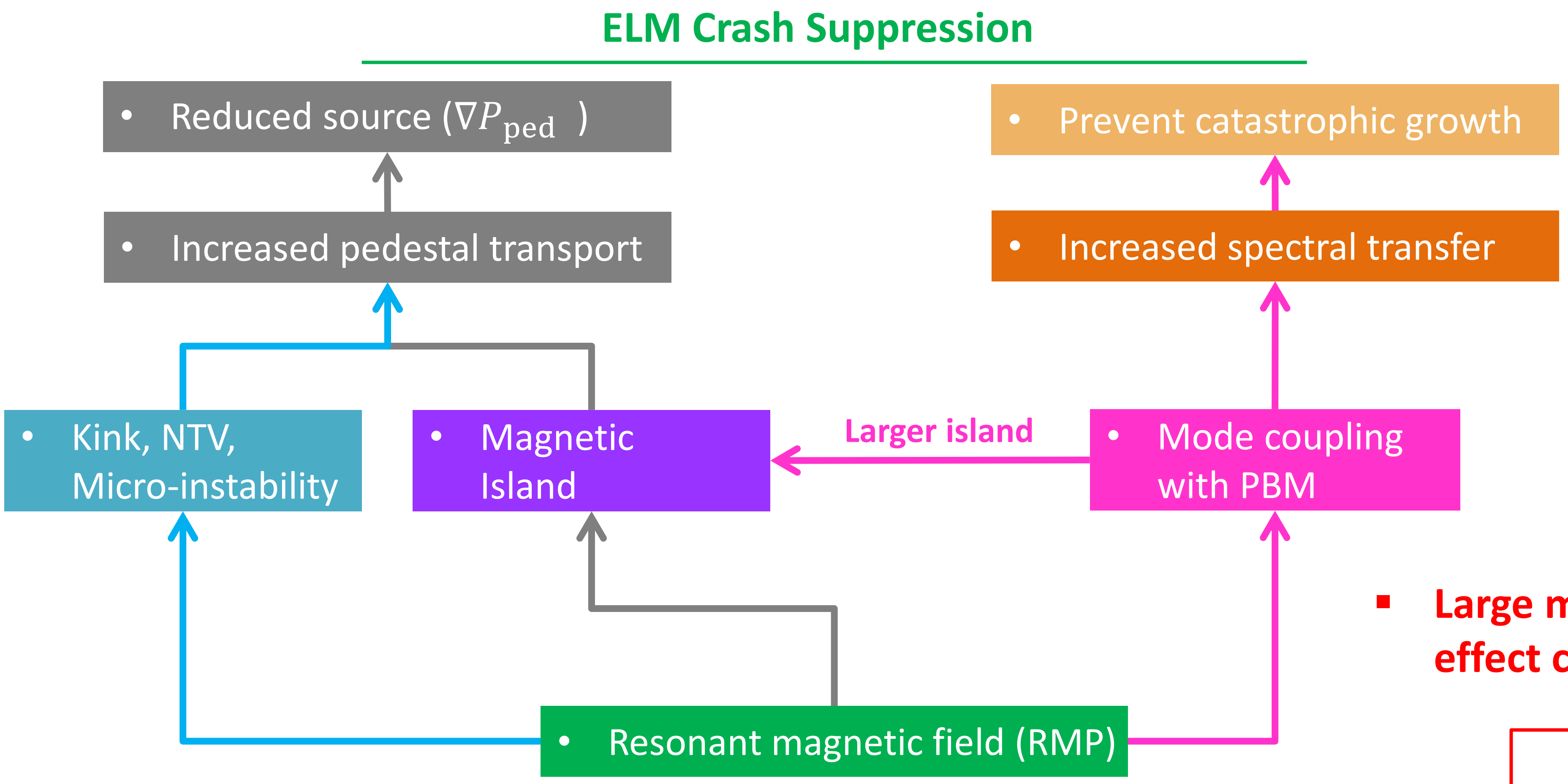

- **Large mode coupling effect can be favorable.**

How?

PBM locking

- **Locking of mode structure**
  - ✓ PBM is locked ($v_{\theta,\mathrm{PBM}} \rightarrow 0$) when suppression is achieved ($I_{\mathrm{RMP}}\sim 4\ \mathrm{kA}$).
  - ✓ Similar trend is observed in the previous experiment [1, 2].
  - ✓ Mode locking (bifurcation) is one of the major differences between mitigation and suppression.
  - ✓ When mode locking occurs, $v_{\theta,\mathrm{PBM}}$ and $v_{\theta,\mathrm{E\times B}}$ are decoupled.

    → $v_{\theta,\mathrm{PBM}}: -3 \rightarrow 0\ \mathrm{km/s}$ while $v_{\theta,\mathrm{E\times B}}: -3 \rightarrow -8\ \mathrm{km/s}$

$$\therefore v_{\theta,\mathrm{PBM,RMP}} = v_{\theta,\mathrm{PBM,woRMP}} + \Delta v_{\theta,\mathrm{RMP}}$$

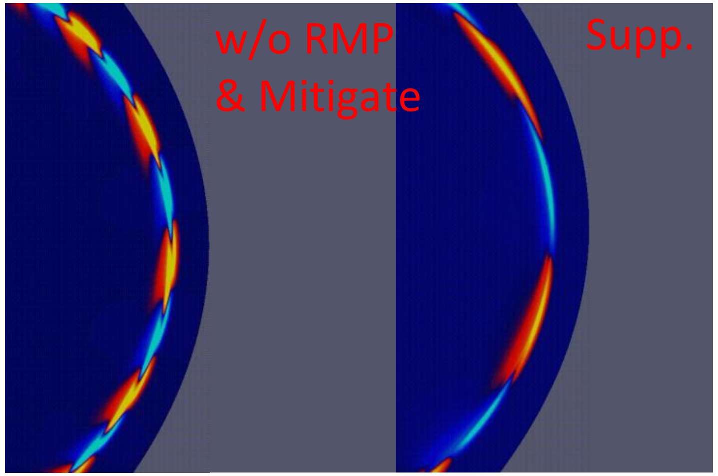

[$v_{\theta,\mathrm{PBM}}$ in ELMy and Suppressed case]

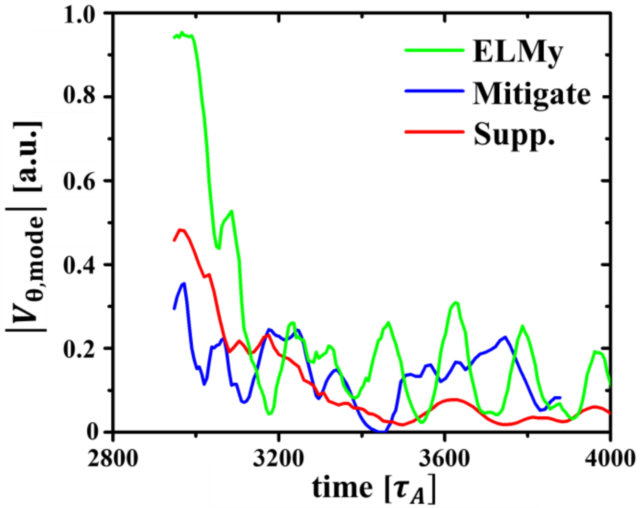

[Time evolution of $v_{\theta,\mathrm{PBM}}$ of dominant n]

[1] J. H. Lee et al., APS (2019, Ft Lauderdale, USA)
[2] R. Nazikian et al, PRL 114 (2015), 105002

PBM locking - Role on the mode coupling

- **PBM locking and mode coupling**
  - ✓ Constant or sustained phase difference ($\Delta\delta$) b/w RMP and PBMs is favorable to strong mode interaction.
    → Keeping the spatial overlapping of mode structures
  - ✓ RMP driven plasma response is static in space.
    → $v_{\theta,\mathrm{PBM}} \approx 0$ for $\Delta\delta \approx$ const.
  - ✓ PBM locking may be difficult to occurs with large $v_{\theta,\mathrm{E\times B}}$ in pedestal.

$$\because\ v_{\theta,\mathrm{PBM,RMP}} \approx v_{\theta,\mathrm{E\times B}} + \Delta v_{\theta,\mathrm{RMP}} \rightarrow 0$$

  - ✓ PBM locking and suppression are not achieved with increase $|v_{\theta,\mathrm{E\times B}}|$.
    → Advantageous small $v_{\theta,\mathrm{PBM}}$ (or $v_{\theta,\mathrm{E\times B}} \rightarrow 0$)

➢ PBM locking can be an advantageous consequence or reason for one branch of ELM suppression

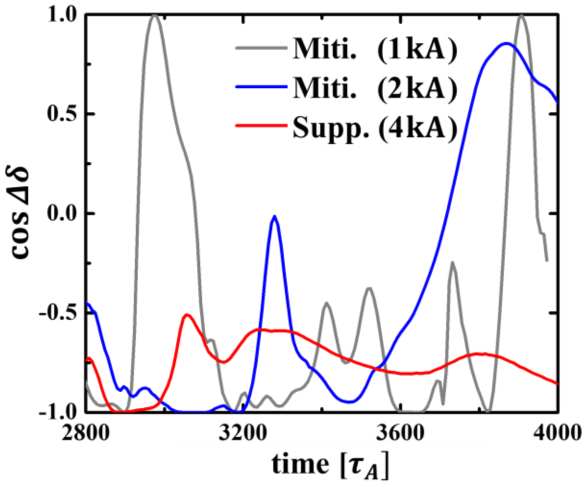

[Time evolution of cos $\Delta\delta$]

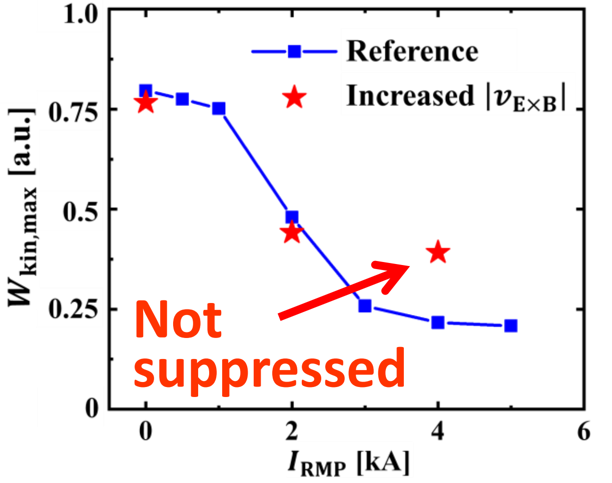

[Mode amplitude for I_{RMP}]

Outline

- Introduction
- Simulation setup
  - Numerical tools & Reference
- RMP driven Plasma response
  - Kink-tearing response
  - Increased pedestal transport
- RMP driven ELM crash suppression
  - Natural & RMP PBM simulation
  - Coupled RMP & PBM
  - PBM locking
- **Conclusion**

RMP simulation with equilibrium — - Equilibrium response

⬇

Natural PBM (w/o RMP) simulation
RMP simulation with PBM — - PBM response

Conclusion - I

- **Nonlinear effect of RMP on the pedestal has been investigated.**

- **Kink-tearing response is observed under RMP**
  - ✓ **Axisymmetric equilibrium change accompanied by Kink + Tearing non-axisymmetric features.**
  - ✓ **Mean (n = 0) pedestal profile degradation (Kink + Tearing)**
    - T **pedestal: Stochastic layer (Tearing part)**
    - n_{e} **pedestal: $\Gamma_{\mathrm{E\times B}}$ Convective flux (Kink part)**

- **Additional transport mechanism is needed to fully explain the pedestal degradation by RMP.**
  - ✓ **NTV & Micro instabilities will play important role.**

Conclusion - II

- Degradation of pedestal gradient may not solely explain ELM suppression.
- ELM is nonlinearly suppressed by RMP.
  - ✓ ELM suppression accompanied by
    - Reduced pedestal pressure gradient.
    - Mode coupling b/w PBMs and n = 2 RMP driven modes.
- Mode coupling b/w ELMs and n = 2 RMP driven modes is important.
  - Increased pedestal transport by enlarging the magnetic island
  - Prevented mode crash by increasing energy transfer b/w harmonics
- Coupling between RMP and ELMs may explain the locked filament structure during the suppression phase in Exp.

Conclusion - III

- PBM locking is distinguished feature of ELM suppression.
  - ✓ Good agreement with experimental observation via ECEI
  - ✓ Strengthened mode coupling b/w RMP and PBM

- Favorable conditions for the mode coupling are
  - ✓ Plasma conditions for the PBM locking.
    - Small $v_{\theta,\mathrm{PBM}} \to 0$ is advantageous.
    - $v_{\theta,\mathrm{E\times B}} \leq v_{\theta,\mathrm{PBM}} \leq v_{\theta,\mathrm{E\times B}} + v_{\theta,\mathrm{i*}}/2$ at linear phase w/o RMP. (Depends on the collisionality and dominant n)

- It may be correlated with the importance of $v_{\theta,\mathrm{E\times B}} \approx 0$ in ELM suppression.

Collaboration with PPPL

- **Integrated simulation with JOREK and PENTRC**
  - ✓ Include NTV in the simulation for the particle and momentum transport.
  - ✓ PENTRC is connected to JOREK for the NTV calculation.
  - ✓ Work is on progress.

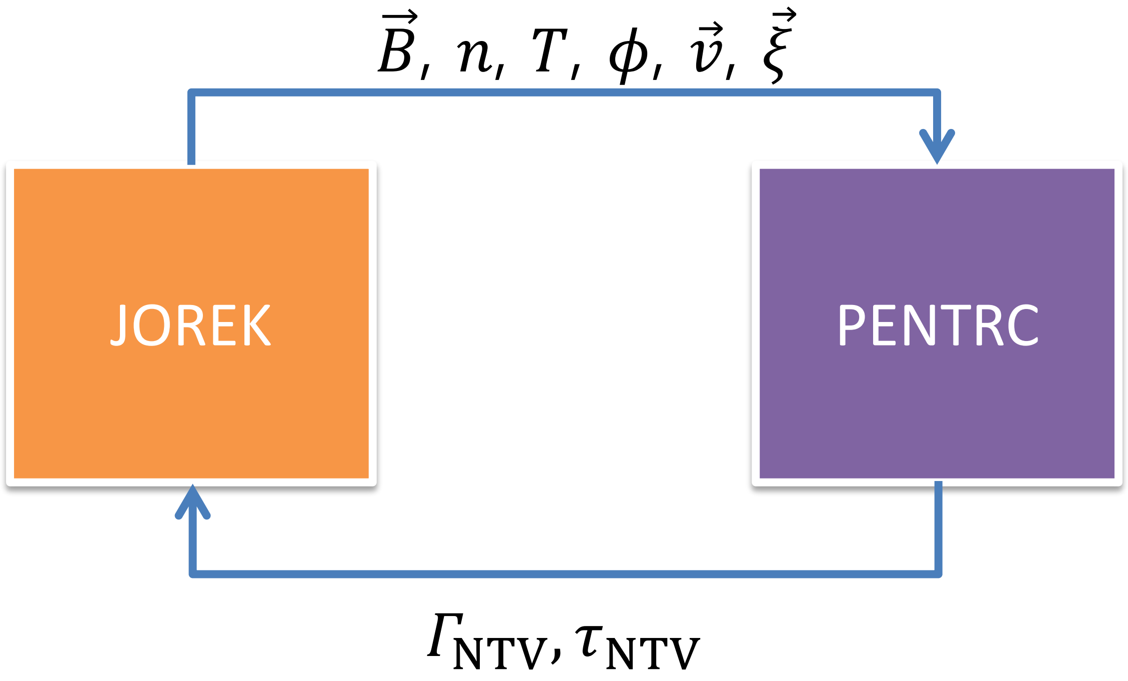

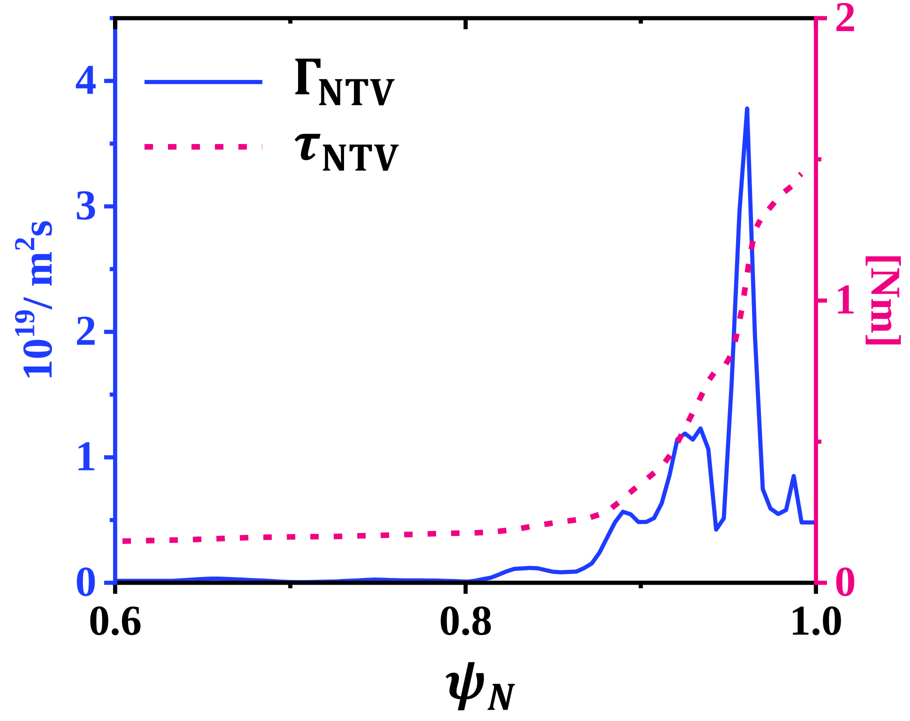

[NTV results, JOREK+PENTRC]

Thank You

Plasma Laboratory for Advanced REsearch

SEOUL NATIONAL UNIVERSITY

National Fusion Research Institute

Backup - RMP driven ELM suppression

- **Bifurcation of poloidal mode rotation**
  - ✓ **Sudden bifurcation of rotation occurs at the suppression phase.**
  - ✓ **The mode rotation becomes very small ($v_{\theta,\mathrm{mode}} \approx 0$).**
  - ➢ **It suggests the possibility of interactions b/w RMP and PBM.**

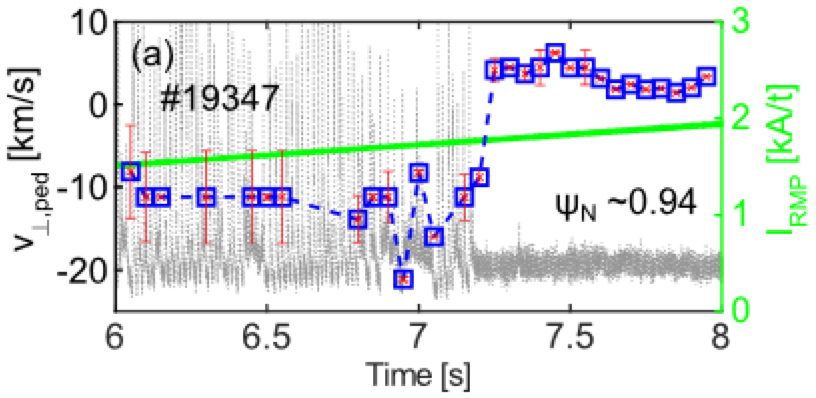

[**Mode locking in suppression,** J.Lee (NF 2019)]

- **Direct effect of RMP on PBMs**
  - ✓ **RMP can directly affect ELM “crash” suppression.**
  - ✓ **Effect of RMP on the PBMs are..**
    - **Linear effect of RMP induced field structure on PBM [1, 2].** ➡ **Linear effect of 3D field on PBM**
    - **Nonlinear MHD simulations on the RMP driven KPM [3] and ELM mitigated/suppressed case [4,5].** ➡ **Nonlinear coupling b/w RMP and PBM**

➢ **NL simulation including both RMP and PBM is needed.**

[1] M. Willensdorfer et al., PRL 119 (2017), 085002
[2] M. L. Mou et al., Phys. Plasma 25 (2018), 082518
[3] F. Orain et al., Nucl. Fusion 57 (2017), 022013
[4] M. Becoulet et al., PRL 113 (2014), 115001
[5] F. Orain et al., Phys. Plasma (2019), 042503

Backup - Limitation of KSTAR EFIT

- **Limitation of KSTAR EFIT**
  - ✓ **There is no standard of "good" EFIT in KSTAR.**
  - ✓ **There are many obstacles to construct a "good" kinetic profile and EFIT.**

Kinetic Profile

- Overall Profile fitting
- Pedestal Profile fitting

- Diagnostics-
- Low resolution
- Uncertainty

EFIT (Equilibrium)

- Kinetic Profile
- Magnetic measurement
- Current profile (MSE)
- Numerical constraint

Magnetic measurement →
- Bad Channels

Current profile (MSE) →

- MSE -
- Uncertainty
- Availability

Numerical constraint →
- Lack of optimized parameters for KSTAR

Backup - Numerical/Theoretical compensation

- **Kinetic profile correction**
  - ✓ **Multi diagnostic based least square fitting**
    - ▪ **Thomson, ECE, Inter/Reflectometry and CES**
  - ✓ **Various numerical filters & function based fitting**
  - ✓ **Theoretical model based pedestal profile**
    - ▪ **ELM toroidal n (n_{ECE}) and ELM size (ΔW_{ELM})**
- **Current profile correction**
  - ✓ **Theoretical model based current profile**
    - ▪ **Synthetic MSE vs Experimental MSE**
    - ▪ **Edge bootstrap current**
- **KSTAR parameter optimization**
  - ✓ **Optimization through brutal force approach**

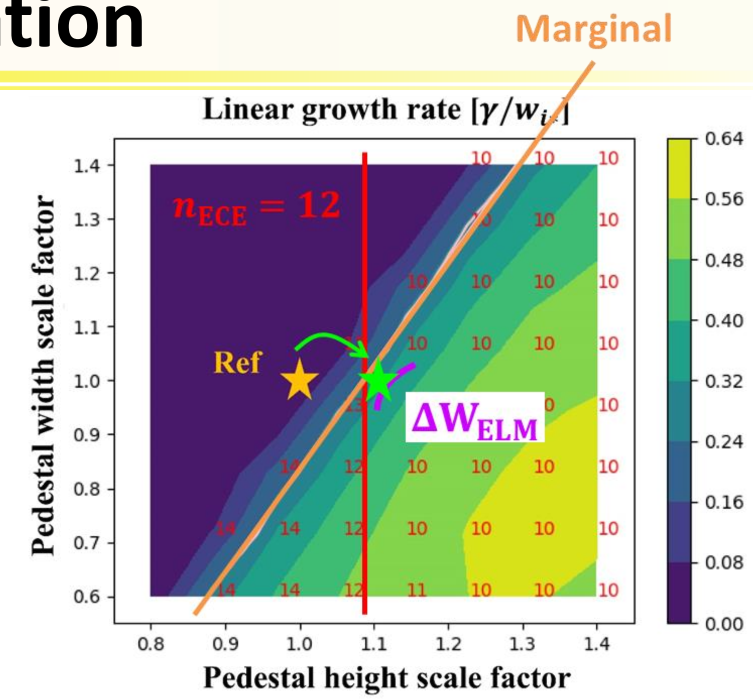

[Model based Pedestal modification]

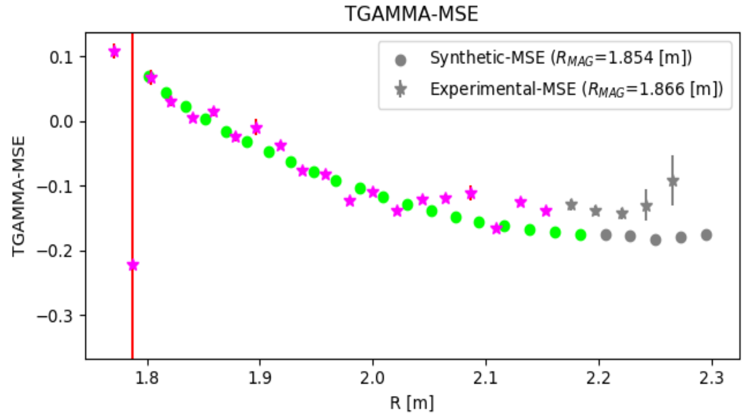

[Experimental vs Simulated MSE]

Backup – reference EFIT

- **Kinetic profile and EFIT construction**
  - ✓ **GFIT & GEFIT package is developed to construct a kinetic profile and EFIT in KSTAR.**
  - ✓ **They are in full production at the KSTAR computing server (one of standard branch).**

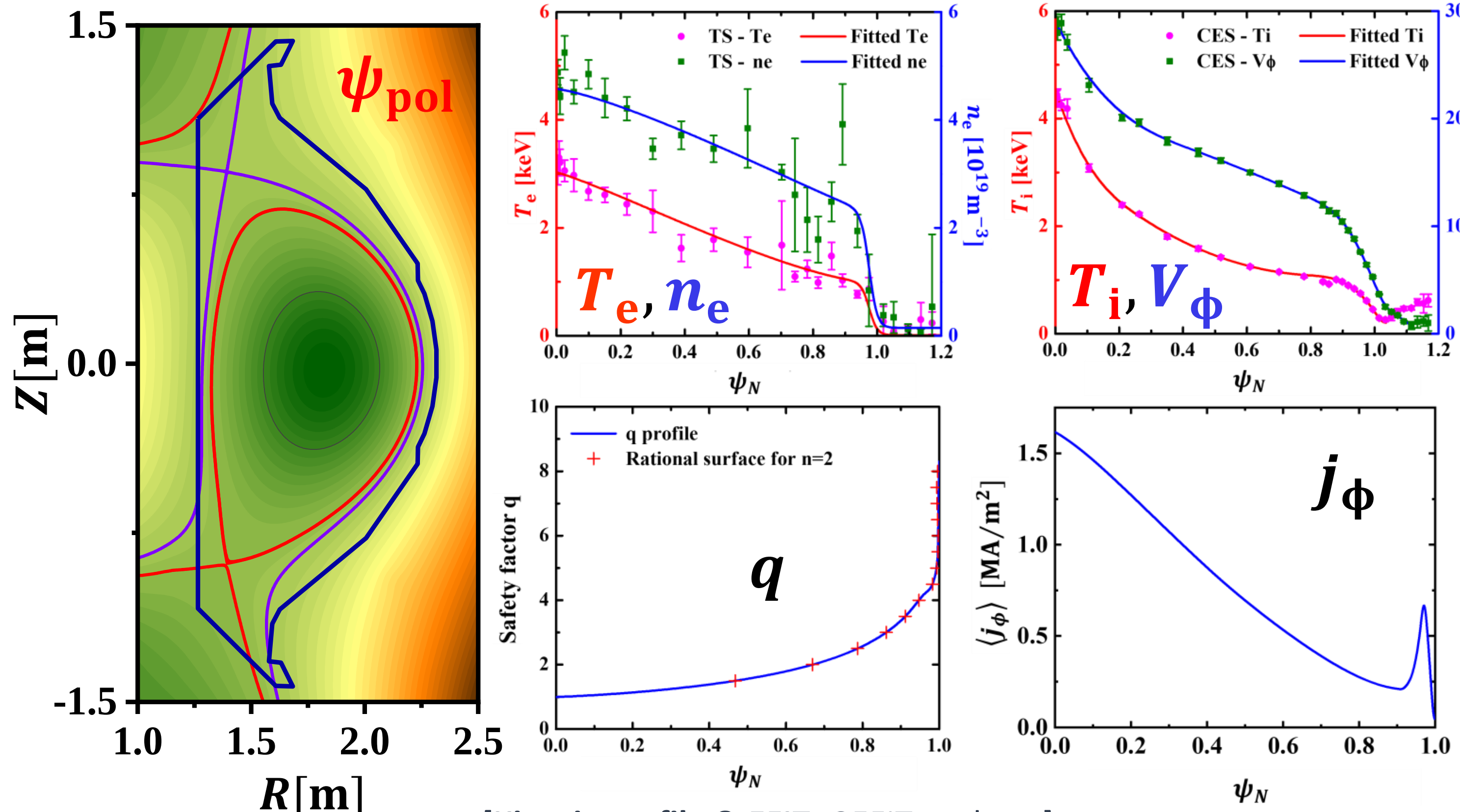

[**Kinetic profile & EFIT,** GEFIT package]

Numerical accuracy	**Convergence:** $\mathbf{10^{-4} \rightarrow 10^{-11}}$
Experimentally relevant	Error: $\mathrm{N/A} \rightarrow \mathbf{14.5}$

➢ **"Good" reference is developed for the simulation.**

Backup - RMP driven ELM crash suppression

- **RMP and divertor heat flux**
  - ✓ Instantaneous ELMy peak heat flux (Q_{peak}) decreases with RMP.
  - ✓ Q_{peak} is drastically reduced for $I_{RMP} \geq 3\text{kA}$ where modes are suppressed.
  - ✓ Background heat flux increases with I_{RMP} due to the enhanced transport to SOL.

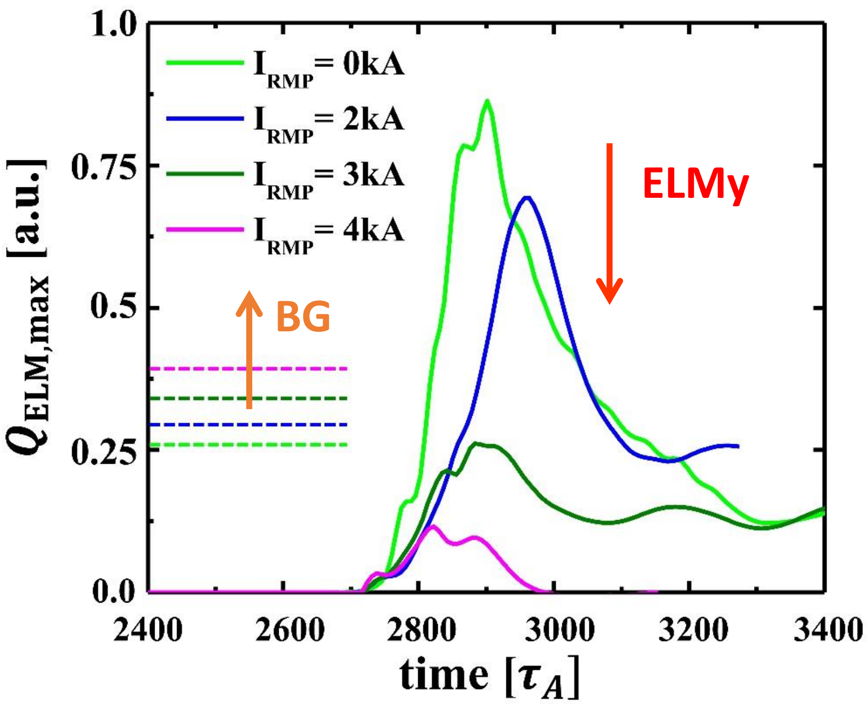

[ELMy peak divertor heat flux induced by PBMs]

➢ PBM suppression is reproduced with experimentally relavent RMP configuration

- **Suppression of PBM with RMP can be related to**
  - Reduced pressure gradient

Backup - Simulation setup

- **Target discharge and equilibrium**
  - ✓ #18594 is selected for the simulation.
  - ✓ $B_T = 1.8$ T, $I_p = 660$ kA, $q_0 \sim 1$, $q_{95} \sim 4$, $\beta_p = 1.0$, $\bar{n}_e = 3.3 \times 10^{19}$ m^{-3}
  - ✓ ELMs are suppressed with n=2 ($\phi = 90°$), $I_p \sim 3.7$ kA RMP configuration [1].
  - ✓ Modified Sauter formula [2] is applied to construct the bootstrap current.

- **Numerical setup**
  - ✓ Neoclassical constraint (v_{neo}) is applied to construct the ion-poloidal flow.
  - ✓ $v_{\theta,E\times B}$ in the pedestal region is in the ion-diamagnetic direction.
  - ✓ $T_i = T_e$ is assumed.
  - ✓ Adaptive diffusive profile and source are used to sustain the ρ, T, v_ϕ profiles.
  - ✓ Spitzer-like resistivity (x40) and braginskii parallel conductivity are used.

$$v_\theta = v_{E\times B} + v_{i*} + v_{||,\theta}$$

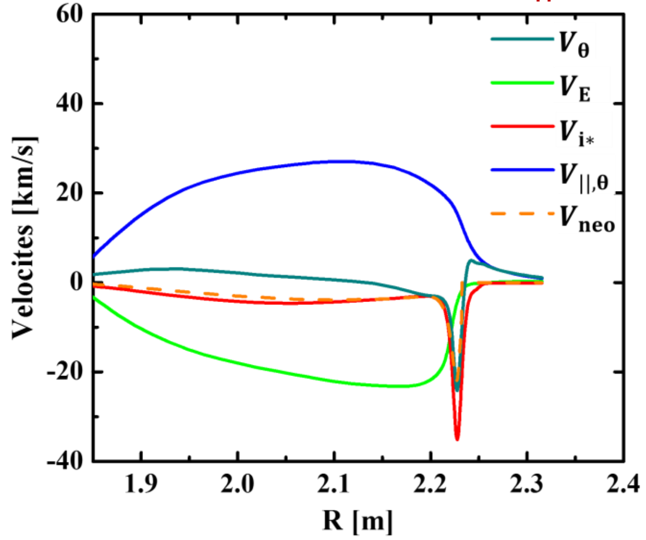

[Poloidal flow components]

[1] Y. M. Jeon et al., PRL 109 (2012), 035004
[2] R. Hager and C. S. Chang et al., Phys. Plasmas 23 (2016), 042503